Behavioral/Cognitive

Behavioral and Neural Dissociation of Social Anxiety and Loneliness

Jana Lieberz,[1] Simone G. Shamay-Tsoory,[2] Nira Saporta,[2] Alisa Kanterman,[2] Jessica Gorni,[1] Timo Esser,[1] Ekaterina Kuskova,[1] Johannes Schultz,[3,4] René Hurlemann,[5,6] and Dirk Scheele[1,5]

[1]Research Section Medical Psychology, Department of Psychiatry and Psychotherapy, University Hospital Bonn, Bonn, 53127, Germany, [2]Department of Psychology, University of Haifa, Haifa, 3498838, Israel, [3]Center for Economics and Neuroscience, University of Bonn, Bonn, 53127, Germany, [4]Institute of Experimental Epileptology and Cognition Research, University of Bonn, Bonn, 53127, Germany, [5]Department of Psychiatry, School of Medicine & Health Sciences, University of Oldenburg, Oldenburg, 26129, Germany, and [6]Research Center Neurosensory Science, University of Oldenburg, Oldenburg, 26129, Germany

Loneliness is a public health concern with detrimental effects on physical and mental well-being. Given phenotypical overlaps between loneliness and social anxiety (SA), cognitive-behavioral interventions targeting SA might be adopted to reduce loneliness. However, whether SA and loneliness share the same underlying neurocognitive mechanisms is still an elusive question. The current study aimed at investigating to what extent known behavioral and neural correlates of social avoidance in SA are evident in loneliness. We used a prestratified approach involving 42 (21 females) participants with high loneliness (HL) and 40 (20 females) participants with low loneliness (LL) scores. During fMRI, participants completed a social gambling task to measure the subjective value of engaging in social situations and responses to social feedback. Univariate and multivariate analyses of behavioral and neural data replicated known task effects. However, although HL participants showed increased SA, loneliness was associated with a response pattern clearly distinct from SA. Specifically, contrary to expectations based on SA differences, Bayesian analyses revealed moderate evidence for equal subjective values of engaging in social situations and comparable amygdala responses to social decision-making and striatal responses to positive social feedback in both groups. Moreover, while explorative analyses revealed reduced pleasantness ratings, increased striatal activity, and decreased striatal-hippocampal connectivity in response to negative computer feedback in HL participants, these effects were diminished for negative social feedback. Our findings suggest that, unlike SA, loneliness is not associated with withdrawal from social interactions. Thus, established interventions for SA should be adjusted when targeting loneliness.

Key words: **amygdala; fMRI; loneliness; social anxiety; striatum**

Significance Statement

Loneliness can cause serious health problems. Adapting well-established cognitive-behavioral therapies targeting social anxiety might be promising to reduce chronic loneliness given a close link between both constructs. However, a better understanding of behavioral and neurobiological factors associated with loneliness is needed to identify which specific mechanisms of social anxiety are shared by lonely individuals. We found that lonely individuals show a consistently distinct pattern of behavioral and neural responsiveness to social decision-making and social feedback compared with previous findings for social anxiety. Our results indicate that loneliness is associated with a biased emotional reactivity to negative events rather than social avoidance. Our findings thus emphasize the distinctiveness of loneliness from social anxiety and the need for adjusted psychotherapeutic protocols.

Received Oct. 8, 2021; revised Jan. 20, 2022; accepted Jan. 21, 2022.

Author contributions: J.L. and D.S. designed research; J.L., J.G., T.E., and E.K. performed research; J.L., J.G., J.S., and D.S. analyzed data; J.L. wrote the first draft of the paper; S.G.S.-T., N.S., A.K., J.G., T.E., E.K., J.S., R.H., and D.S. edited the paper.

S.G.S.-T., R.H., and D.S. were supported by German-Israel Foundation for Scientific Research and Development Grant GIF I-1428-105.4/2017. D.S. was also supported by an Else-Kröner-Fresenius-Stiftung grant (2017_A35). We thank Alexandra Goertzen-Patin for proofreading the manuscript; and Marie Coenjaerts and Mitjan Morr for helpful discussions about the manuscript.

The authors declare no competing financial interests.

Correspondence should be addressed to Jana Lieberz at jana.lieberz@hotmail.de or Dirk Scheele at dirk-scheele@gmx.de.

https://doi.org/10.1523/JNEUROSCI.2029-21.2022

Introduction

Loneliness is a painful condition with detrimental effects on mental and physical health (Quadt et al., 2020). As such, loneliness has been identified as a risk factor for premature mortality comparable with smoking or obesity (Holt-Lunstad et al., 2010). Consequently, loneliness has come into focus of politics and clinicians as a major public health concern with high economic costs for society (Jeste et al., 2020; Mihalopoulos et al., 2020). With social distancing measures in most countries around the world, COVID-19 is expected to have vast impact on physical and mental health, particularly in people inflicted by poor

resilience to social adversity because of preexisting low levels of social integration (Galea et al., 2020; Vindegaard and Benros, 2020), emphasizing the urgent need of interventions to target loneliness. Adjusting established cognitive-behavioral therapies targeting-related psychopathology, such as depression or social anxiety (SA) (Heinrich and Gullone, 2006), seems promising to accelerate the development of treatments to reduce loneliness. However, previous studies indicated that loneliness and depression are distinct constructs based on unique neurobiological mechanisms (Cacioppo et al., 2010; Shao et al., 2019). Conversely, it is still unclear whether loneliness shares neurobiological substrates with SA, which would allow rapid co-optations of psychotherapeutic protocols.

Recent findings highlight close links between loneliness and SA symptoms (Bruce et al., 2019; Maes et al., 2019) and identified SA as predictor for future loneliness (Lim et al., 2016; Danneel et al., 2019). For instance, SA was found to be consistently associated with social isolation, lower perceived social support, and poor friendship quality, resulting in decreased relationship satisfaction, which is a key feature of loneliness (Peplau and Caldwell, 1978; Teo et al., 2013; Porter and Chambless, 2014; Rapee et al., 2015; Rodebaugh et al., 2015). Likewise, the avoidance of social situations is known to be a core mechanism of SA; and although loneliness might have evolved as a motivation to reconnect with others, social avoidance is also hypothesized to be preferred by lonely individuals (Cacioppo and Cacioppo, 2018).

Existing SA intervention programs are often based on cognitive models of SA (Clark and Wells, 1995), which posit an exaggerated fear of evaluation as a core etiologic mechanism of psychopathology. Indeed, current neurocircuitry models of SA disorder emphasize amygdala hyperreactivity to social stimuli (Etkin and Wager, 2007; Bruhl et al., 2014). Conversely, the neural responsiveness to social rewards seems to be reduced in individuals with SA (Richey et al., 2017; Schultz et al., 2019), potentially resulting in reduced positive affect in response to social interactions (Kashdan and Collins, 2010). Similarly, lonely individuals exhibit attenuated responsiveness to positive social interactions (Lieberz et al., 2021), and preliminary evidence indicates that alterations in amygdala structure and function are associated with loneliness (for a comprehensive review of neurobiological correlates of loneliness, see Lam et al., 2021; Morr et al., 2022).

The current study therefore aims at examining whether mechanisms underlying SA could also underlie loneliness. We recruited a prestratified sample of 42 healthy participants with high (high-lonely [HL]) and 40 participants with low (low-lonely [LL]) loneliness scores. During fMRI, the participants completed a social gambling task as used by Schultz et al. (2019) to measure the behavioral and neural responsiveness to social decision-making and social feedback. Given the intertwined phenotype of SA and loneliness, we hypothesized that lonely individuals would show increased SA symptomatology and in turn behavioral and neural response patterns associated with social avoidance (compare Schultz et al., 2019). Specifically, we hypothesized decreased subjective values of engaging in social situations, increased amygdala activation during social decision-making and social feedback, and decreased reward-associated responses of the nucleus accumbens (NAcc) to positive social feedback in lonely participants. Moreover, we explored distinct behavioral and neural response patterns in loneliness that have not been previously found to be associated with SA (i.e., responsiveness to negative social feedback). We controlled for the influence of SA and further potential confounding variables for all observed correlates of loneliness.

Materials and Methods

Participants. We recruited a sample of 82 (of a stratified sample of 3678 adults; 41 females, mean age ± SD: 26.83 ± 7.47 years) (see Lieberz et al., 2021) prestratified healthy HL ($n = 42$) and LL volunteers ($n = 40$) as assessed by the revised version of the UCLA loneliness scale (UCLA-L) (Russell et al., 1980). HL Participants were characterized by UCLA-L scores of ≥50 (i.e., at least 1 SD above the mean score of students) (compare Russell et al., 1980), whereas LL participants were characterized by scores of ≤25 (i.e., at least 1 SD below the mean score of young adults). All participants fulfilled the following inclusion criteria: aged 18-65, no current physical or psychiatric disorder as assessed via self-disclosure and by the Mini-International Neuropsychiatric Interview (Sheehan et al., 1998), no psychotherapy, no current psychotropic medication, no illicit drug use in the previous 4 weeks, right-handed, and eligibility for MRI scanning. The sample size was based on an *a priori* power analysis (compare Lieberz et al., 2021). The analysis using G*Power 3 (Faul et al., 2007) indicated that at least 71 participants were needed to reliably replicate a previously reported loneliness effect on ventral striatum/amygdala activity (Cacioppo et al., 2009) with a power of 0.99 ($\alpha = 0.05$). To account for possible missing data and dropouts, we planned to test at least 80 participants, resulting in the final sample size of 82 participants. For a comprehensive description of the prestratification approach, see Lieberz et al. (2021).

All participants gave written informed consent. The study was approved by the institutional review board of the Medical Faculty of the University of Bonn (study number 016/18) and conducted in accordance with the latest revision of the Declaration of Helsinki.

Experimental design and statistical analyses. Following the screening of inclusion criteria, participants completed a virtual auction task to measure the individual monetary value associated with receiving positive or avoiding negative social feedback. To further measure the participants' subjective value of engaging in social situations, participants competed a social gambling task (compare Schultz et al., 2019) during a separate test session and repeated the task during fMRI on the same day. Data collection was completed before the start of the COVID-19 pandemic. The analysis plan was preregistered before conducting any analyses (https://osf.io/x47ke). All data used in this study are openly available (https://osf.io/p6jxk/ and https://neurovault.org/collections/VNYRMORR/).

Social gambling task. Each trial of the social gambling task consisted of a decision and a feedback stage (Fig. 1). During the decision phase, participants could choose a risky (a dice game with a virtual human or computer partner with equiprobable outcomes of 3 or 0 €) or a safe option (a fixed payoff ranging from 0 to 3 € in steps of 50 cents) with no imposed time limit. Human partners were indicated by the name and picture of 1 of 4 partners, while the computer control condition was indicated by a picture of a computer. If participants chose the risky option, either a positive or a negative feedback video of the partner (human or computer) was shown (feedback phase), depending on the outcome of the trial (win or loss). As such, the human feedback video displayed the virtual human partner expressing either admiration or condescension. All human pictures and videos were taken from a validated database (Kaulard et al., 2012). In the computer control condition, the feedback was given by a video of a checkmark (participant won) or a cross (participant lost). Each feedback video was presented 2 times in immediate succession. If participants chose the safe option, a sentence confirmed the payoff. Each human partner was paired twice with each possible amount of money offered as alternative for the risky option, resulting in 56 trials. Likewise, participants completed 56 trials of the control condition. After finishing the task, participants rated the pleasantness of each positive and negative feedback video on a visual analog scale ranging from 0 ("not pleasant at all") to 100 ("very pleasant"). Moreover, for each participant, individual certainty equivalents of the risky option (termed CE50, i.e., the certain payoff for which a participant would be indifferent between the risky and safe options: they would

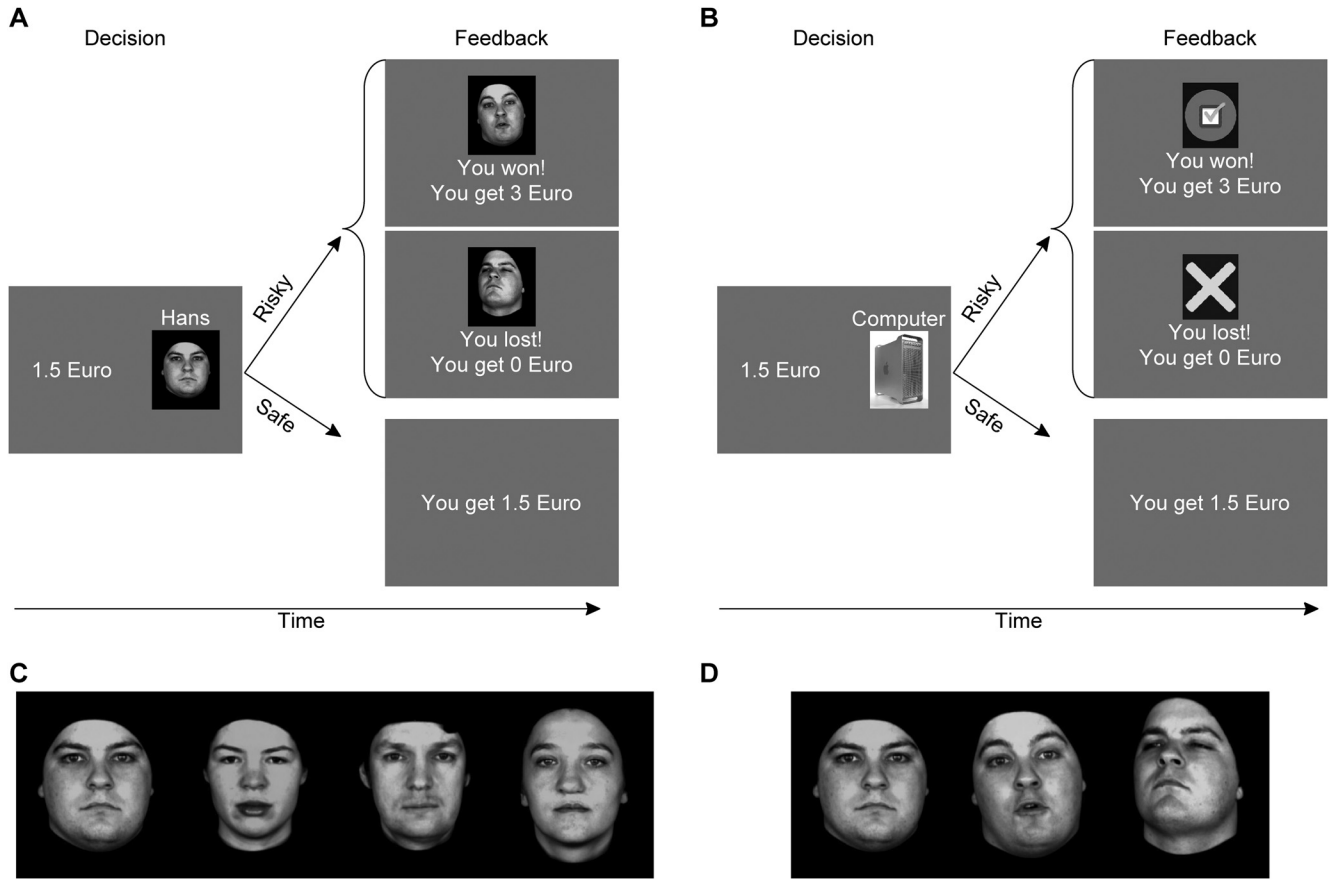

Figure 1. Social gambling task. The social gambling task included a human (***A***) and a computer (***B***) condition, and each trial consisted of a decision and a feedback stage. During the decision phase, participants could choose a risky or a safe option (a uniformly distributed random fixed payoff ranging from 0 to 3 € in steps of 50 cents). If participants chose the risky option and won the trial, a positive feedback video of the partner was shown and the participant got 3 €. If participants lost the trial, they received no payoff and a negative feedback video was presented. The human feedback video displayed the virtual human partner expressing either admiration (participants won) or condescension (participant lost). In the computer control condition, the feedback was given by a video of a checkmark (participant won) or a cross (participant lost). If participants chose the safe option, a sentence confirmed the payoff. During fMRI, the partner was indicated by the name of the virtual human partner or the word "computer" only. ***C***, The four virtual human partners with neutral facial expression. ***D***, One of the partners with neutral, admiring, and condescending facial expressions (left to right). The admiring and condescending expressions were presented as videos during the feedback stage. See also Schultz et al. (2019, their Fig. 1).

choose each option with equal probability) were estimated separately for the computer and the human partners by fitting participants' choices as a function of the difference between the expected values of the safe and risky options with a cumulative Gaussian function. CE20 and CE80 (i.e., certain payoffs associated with choosing the safe option with 20% and 80%, respectively, probability) were similarly estimated. The subjective value of engaging in social situations was defined as the individual difference between the estimated CE50 for human partners compared with the computer partner.

The task was repeated during fMRI with the following adjustments: the partner for each trial (1 of 4 human partners or the computer) was chosen randomly and indicated by the name of the partner (no face was shown at this stage) or the word "computer." Furthermore, the fixed payoff offered in the safe option varied randomly between the three individually determined values CE20, CE50, and CE80. Using individualized payoffs as a safe alternative enabled us to equate the number of risky and safe choices across participants. Participants responded with their index fingers using an MRI-compatible response grip system (NordicNeuroLab). The position of the risky option (left or right on the screen) was counterbalanced across trials. All human partners were presented in combination with each of the three CE values twice, resulting in 24 human trials and 24 computer trials per run. The feedback video was presented 2 times during a fixed time interval of 2.6 s. The temporal intervals between the decision and outcome stages and the interstimulus intervals between trials varied from 2 to 11 s with a descending probability. All participants completed two runs. Participants received the obtained money from one randomly chosen trial per run. To summarize, this task allowed us to obtain an experimental measure of social avoidance behavior (specifically, the difference in subjective values between engaging in an interaction with a person or a computer) and its associated neural signal (amygdala hyperactivity during social decision-making, amygdala hypersensitivity to human feedback, and reduced reward-associated brain activity in response to positive human feedback). Thus, the task enabled us to concurrently explore behavioral and neural response patterns associated with social avoidance and social feedback processing as core mechanisms underlying the persistence of SA.

Virtual auction task. We further measured the individual monetary value associated with receiving positive or avoiding negative social feedback during a virtual auction task. Specifically, participants were informed that they were participating in a virtual auction against the computer using a random algorithm to invest money. In each trial, a picture of one of six actors indicated which feedback video was being auctioned. The same actors and videos as included in the social gambling task were used plus two additional actors from the same database (see above). In each trial, participants were asked with no imposed time limit to invest any amount of money between 0 € and 1 € at their disposal (in increments of 5 cents) to (1) increase the probability of watching a positive social feedback video or (2) to decrease the probability of watching a negative social feedback video. There were six trials in the positive and six trials in the negative feedback conditions. After completion of all

trials, one trial was chosen randomly and the invested money was compared with a randomly selected amount representing the money invested by the computer. The player (participant or computer) who invested more money won the auction, received the outcome of the trial, and kept the remaining money (1 € minus the invested money). As the investments of the computer were based on uniformly distributed random investments between 0 € and 1 €, each cent invested by the participant corresponded to a probability change of 1% to win the auction. In the positive feedback condition, a positive social feedback video (expressing admiration) was presented if the participant won the auction, while no video was presented if the participant lost. In the negative feedback condition, a negative social feedback video (expressing condescension) was presented if the participant lost and no video was shown if the participant won. If the participants lost, they kept 1 €, regardless of the invested money. The feedback videos were repeated until the participants pressed any key. Notably, winning the auction was associated with a smaller monetary payout than losing the auction. This way, the virtual auction task enabled us to explore whether receiving positive social feedback or avoiding negative feedback would be worth a higher monetary loss for HL compared with LL participants.

fMRI data acquisition and preprocessing. All fMRI data were acquired using a 3T Siemens TRIO MRI system (Siemens) with a Siemens 32-channel head coil. Functional data of the social gambling task were acquired using a T2*-weighted EPI sequence with a TR of 2500 ms, a TE of 30 ms, ascending slicing, a matrix size of 96×96, 37 axial slices with a voxel size of $2 \times 2 \times 3$ mm^3 and a slice thickness of 3.0 mm, a distance factor of 10%, an FOV of 192×192 mm^2, and a flip angle of 90°. High-resolution T1-weighted structural images were collected on the same scanner (TR = 1660 ms, TE = 2.54 ms, matrix size: 256×256, voxel size: $0.8 \times 0.8 \times 0.8$ mm^3, slice thickness = 0.8 mm, FOV = 256×256 mm^2, flip angle = 9°, 208 sagittal slices). To control for inhomogeneity of the magnetic field, fieldmaps were obtained for the T2*-weighted EPI sequence (TR = 392 ms, TE [1] = 4.92, TE [2] = 7.38, matrix size: 64×64, voxel size: $3 \times 3 \times 3$ mm^3, slice thickness = 3.0 mm, distance factor = 10%, FOV = 192×192 mm^2, flip angle = 60°, 37 axial slices). For preprocessing, standard procedures of SPM12 (Wellcome Trust Center for Neuroimaging; https://www.fil.ion.ucl.ac.uk/spm/) implemented in MATLAB (The MathWorks) were used. The first five volumes of each functional time series were removed to allow for T1 signal equilibration before affine registration was used to correct for head movements between scans. Images were initially realigned to the first image of the time series and then re-realigned to the mean of all images. For unwarping, the voxel displacement map (VDM file) was applied to the EPI time series to correct for signal distortion based on B0-field inhomogeneity. Normalization parameters as determined by segmentation and nonlinear warping of the structural scan to reference tissue probability maps in MNI space were applied to all functional images. All images were resampled at $2 \times 2 \times 2$ mm^3 voxel space and spatially smoothed by using a 6 mm FWHM Gaussian kernel. A high-pass filter with a cutoff period of 128 s was used to detrend raw time series.

Behavioral data analysis. Behavioral data were analyzed in SPSS 24 (IBM). Specifically, to analyze the social gambling task, we calculated mixed-design ANOVAs with the estimated CE50 values, the proportion of safe decisions during the behavioral and the fMRI task, and the pleasantness ratings of the feedback videos as dependent variables. For all analyses, group (HL vs LL) served as between-subject factor and the partner condition (human vs computer) was included as within-subject factor. Offered payoffs as safe option were further included as within-subject factor for the behavioral task (0-3 € in steps of 50 cents) and the fMRI task (CE20, CE50, CE80) to analyze the proportion of safe decisions, whereas the analysis of the pleasantness ratings of the feedback videos included the additional within-subject factor feedback valence (positive vs negative feedback). For task validation, we first tested whether we were able to replicate task effects reported by Schultz et al. (2019). Thus, we examined whether increasing safe option payoffs were associated with increased proportions of safe decisions in both behavior and fMRI tasks (main effect of payoff), and whether positive feedback was rated as more pleasant compared with negative feedback (main effect of feedback valence). Moreover, we tested whether we could replicate the previously observed negative association between SA (measured by the Liebowitz Social Anxiety Scale [LSAS]) (Liebowitz, 1987) and social engagement in participants unaffected by loneliness (i.e., the LL group). We then examined the hypothesized effects of loneliness on the subjective value of engaging in social situations and explored loneliness effects on the pleasantness ratings of the feedback videos.

For the analysis of the virtual auction task, effects of the valence (positive vs negative video) and group were included as within- and between-subject factors, respectively, in a mixed-design ANOVA with invested money serving as dependent variable. Greenhouse–Geisser corrections were applied in cases of violated assumptions of sphericity as tested by Mauchly's test. All *post hoc t* tests to disentangle interactions were Bonferroni-corrected (p_{cor}). p values < 0.05 (two-tailed) were considered significant.

fMRI data analysis. To analyze the fMRI data, we used a two-stage approach as implemented in SPM12. On the first level, data were modeled using a fixed-effects model. Onsets and durations of eight conditions (risky decision computer, safe decision computer, risky decision human, safe decision human, positive computer feedback, negative computer feedback, positive human feedback, and negative human feedback) were modeled by a stick function convolved with an HRF. Although individual CE values were used during the fMRI task to equalize the number of trials of each condition between both runs, the decisions of the participants and thereby the resulting number of trials of one condition still differed between runs to varying degrees. We thus decided to concatenate time series of both runs (compare Cho et al., 2021). Baseline regressors were added for each run, and the high-pass filter and temporal nonsphericity estimates were adjusted separately for each run. The six movement parameters were included in the design matrix as regressors of no interest. Within-subject contrasts of interest were calculated on the first level and entered to a random-effects model on the second level. For task validation, one-sample *t* tests were calculated across groups (i.e., decision human > decision computer, risky decision human > risky decision computer, safe decision human > safe decision computer, human feedback > computer feedback, positive feedback > negative feedback). Furthermore, whole-brain task effects (e.g., decision human > decision computer) were analyzed across groups after applying an initial cluster-forming height threshold of $p < 0.001$. Additional whole-brain analyses were calculated to examine neural responses during decision-making (risky decision vs safe decision) and feedback processing (positive vs negative human feedback) in the social gambling task. To further validate whether the previously observed association between SA and increased amygdala activation during social decision-making (risky decision human > safe decision human and risky decision human > risky decision computer) and while receiving human feedback (human feedback > computer feedback) could be replicated in our sample, we extracted parameter estimates of the anatomically defined amygdala for these contrasts and correlated the averaged activity across voxels with SA scores. Likewise, we analyzed the association between SA and increased NAcc response to positive human compared with positive computer feedback. To ensure that a replication of SA-related findings was not driven by loneliness, we included only participants of the LL group in this analysis.

We then assessed group-specific response patterns by calculating two-sample *t* tests. Specifically, to probe the hypothesis of increased amygdala activation during social decision-making in HL participants, we compared brain activity during risky decisions involving a human partner between groups (i.e., $HL_{\text{risky decision human} > \text{safe decision human}} > LL_{\text{risky decision human} > \text{safe decision human}}$, $HL_{\text{risky decision human} > \text{risky decision computer}} > LL_{\text{risky decision human} > \text{risky decision computer}}$). Likewise, the hypothesized increased amygdala responsiveness to human feedback ($HL_{\text{human feedback} > \text{computer feedback}} > LL_{\text{human feedback} > \text{computer feedback}}$) and reduced NAcc reactivity to positive human feedback ($LL_{\text{positive human feedback} > \text{positive computer feedback}} > HL_{\text{positive human feedback} > \text{positive computer feedback}}$) were tested. As the behavioral data indicated an altered responsiveness to negative human feedback (see Behavioral results), we explored group differences in response to negative human feedback ($HL_{\text{negative human feedback} > \text{negative computer feedback}} > LL_{\text{negative human feedback} > \text{negative computer feedback}}$). These contrasts were also calculated in the opposite

direction (e.g., LL $_{\text{risky decision human}} >$ $_{\text{risky decision computer}} >$ HL $_{\text{risky decision human}} >$ $_{\text{risky decision computer}}$). The amygdala and NAcc were anatomically defined according to the Wake Forest University PickAtlas (Maldjian et al., 2003, 2004). p values < 0.05 after familywise error (FWE) correction for multiple testing (p_{FWE}) based on the size of the respective ROI were considered significant. Additional explorative whole-brain analyses were calculated to compare brain activation between groups for the contrasts of interest. Parameter estimates of clusters showing significant group effects were extracted and further analyzed in SPSS 24 to disentangle the group × task condition interaction. Behavioral group effects were correlated with parameter estimates of neural group effects by calculating Pearson's product-moment correlations. Five participants were excluded from fMRI analyses because of excessive head movement (>4 mm/° in any direction; $n = 2$), anatomic abnormalities ($n = 1$), technical issues ($n = 1$), or incomplete data ($n = 1$). Furthermore, 3 participants were excluded from analyses of the decision stage as they always chose the risky option for at least 1 of the partners, while 1 participant was excluded from analyses of the feedback stage because no positive human feedback was shown during both runs.

Multivariate pattern analysis. We conducted a multivariate pattern analysis using the Decoding Toolbox (Hebart et al., 2014) as further task validation and to probe the replicability of the previous finding that decisions of the participants could be decoded from amygdala activation (compare Schultz et al., 2019). Notably, rather than reanalyzing the involvement of the amygdala in social decision-making as examined by the univariate task validation, the multivariate pattern analysis was used to verify the involvement of the amygdala in decision-making processes regardless of the specific partner (human or computer). For the decoding analysis, we used non-normalized and unsmoothed data of each participant and included the same conditions and regressors as outlined above in the single-subject fixed-effects models separately for both runs. The participants' decisions (risky or safe decision) were used as independent variables, and parameter estimates of the corresponding first-level regressors were used as features. Using the default parameters of the Decoding Toolbox, we ran a classification searchlight analysis with a 9 mm searchlight radius and trained a support vector machine classifier (LIBSVM) on the data of one run to decode the decision to play or to choose the safe option. The decoding accuracy was tested on the data of the other run, and the resulting individual accuracy maps minus chance (chance = 50% accuracy) were normalized to MNI space and smoothed using a 6 mm FWHM Gaussian kernel. Maps of accuracy minus chance decoding performance were then entered into a random-effects model on the second level and tested against 0 by calculating a one-sample t test across groups. FWE correction was applied based on the size of the anatomically defined amygdala (compare Schultz et al., 2019). Furthermore, we explored whether the amygdala activation-based decision decoding accuracy during general decision-making (i.e., across human and computer partners) differed between groups by calculating a two-sample t test.

Functional connectivity analyses. Given that social decision-making and the processing of social rewards rely on complex neural networks rather than on single brain regions (Ruff and Fehr, 2014) and given previously reported associations between SA and altered functional connectivity between the involved brain regions (i.e., amygdala or NAcc) and other brain regions (Schultz et al., 2019), we searched for loneliness-related changes in functional connectivity with the same seed regions (amygdala or NAcc) and other brain regions. Contrasts revealing significant group effects in the univariate activity analyses (see above) were thus examined by exploratory generalized psychophysiological interaction (gPPI) analyses using the CONN toolbox 19.b (www.nitrc.org/projects/conn, RRID:SCR_009550). Following the recommendations of the CONN toolbox, preprocessing for the gPPI analyses additionally included a denoising pipeline. Outlier scans were detected by the integrated artifact detection toolbox-based identification using conservative settings (i.e., thresholds of 0.5 mm framewise displacement and 3 SDs above global BOLD signal changes were used) and treated as regressors of no interest in the following analyses. The default denoising pipeline implemented a linear regression of confounding effects of the first five principal noise components from white matter and CSF template masks, 12 motion parameters, scrubbing, and constant task-related effects. A high-pass filter of 0.008 Hz was applied to minimize the effects of physiological and motion-related noise. Regions associated with group effects (amygdala or NAcc) served as seed regions in a seed-to-voxel analysis. The interaction terms of the psychological (task conditions convolved with a canonical HRF) and the physiological factor (blood oxygenation level-dependent signal) were computed for each participant on the first level. The relative measure of connectivity compared with the implicit baseline was calculated by using bivariate regression measures. Connectivity was compared between groups on the second level by using mixed-design ANOVAs.

Bayesian analyses. The main purpose of the current study was to investigate whether HL participants differ from LL participants in variables associated with core etiologic mechanisms of SA. While frequentist analyses allow to interpret the significance of an observed group difference, a nonsignificant result cannot be interpreted as evidence for the equivalence of groups (Keysers et al., 2020). However, evidence for comparable neural responses to social stimuli and during social decision-making in HL and LL participants would have important clinical implications as this would indicate that loneliness is not associated with neurobiological mechanisms of SA, which are the targets of cognitive-behavioral therapy manuals. Importantly, Bayesian analyses are able to distinguish between the absence of evidence (i.e., more data are needed to interpret the results) and evidence for the absence of an effect and are thus recommended to complement frequentist analyses (Keysers et al., 2020). Therefore, for all hypothesized differences between HL and LL participants that could not be confirmed by classical inference analyses, Bayesian t tests were conducted to quantify the evidence for the null hypotheses (i.e., HL participants do not differ from LL participants) using the default settings for two-tailed independent t tests implemented in JASP (JASP Team, 2020). Specifically, group differences in the subjective value of engaging in social situations during the social gambling task (i.e., the individual CE50 for human partners minus CE50 for the computer partner) and pleasantness ratings of positive human feedback (minus the ratings of positive computer feedback) were reanalyzed by calculating Bayesian t tests. Moreover, as we expected HL participants to differ from LL participants regarding amygdala responsiveness to risky decisions involving a human partner, parameter estimates of the anatomically defined amygdala response during the decision stage were averaged across all voxels and reanalyzed to quantify evidence of differences between groups for the following contrasts of interest: risky decision human > risky decision computer and risky decision human > safe decision human. Likewise, parameter estimates of activation during the feedback stage were extracted from the amygdala to reanalyze responsiveness to human feedback (compared with computer feedback). To reanalyze reward-associated brain activity in response to positive human feedback (compared with computer feedback), parameter estimates were extracted from the NAcc.

Mediation and moderation analyses. For variables that were found to be associated with SA in the LL group, we calculated moderation analyses to investigate whether group (HL vs LL) moderated the size of SA effects. A significant interaction between group and SA would thus indicate that the association between SA and the dependent variable would differ between HL and LL participants. Moderation analyses were calculated for amygdala activation during social decision-making (risky decision human > safe decision human and risky decision human > risky decision computer) and for the subjective values of engaging in social situations as dependent variables, SA scores as independent variable, and group as moderator. Again, parameter estimates were averaged across all voxels of the anatomic amygdala.

Likewise, we conducted moderation analyses to examine whether the differences in negative feedback processing between HL and LL participants differed as a function of SA (i.e., whether the associations between loneliness and the dependent variables were weakened or enhanced for participants with high SA scores). Thus, group (HL or LL) was used as independent variable to analyze those dependent variables that showed differences between groups, and SA was included as moderator variable. In addition to the investigation of interaction effects between group and SA, we examined whether the observed differences between HL and LL

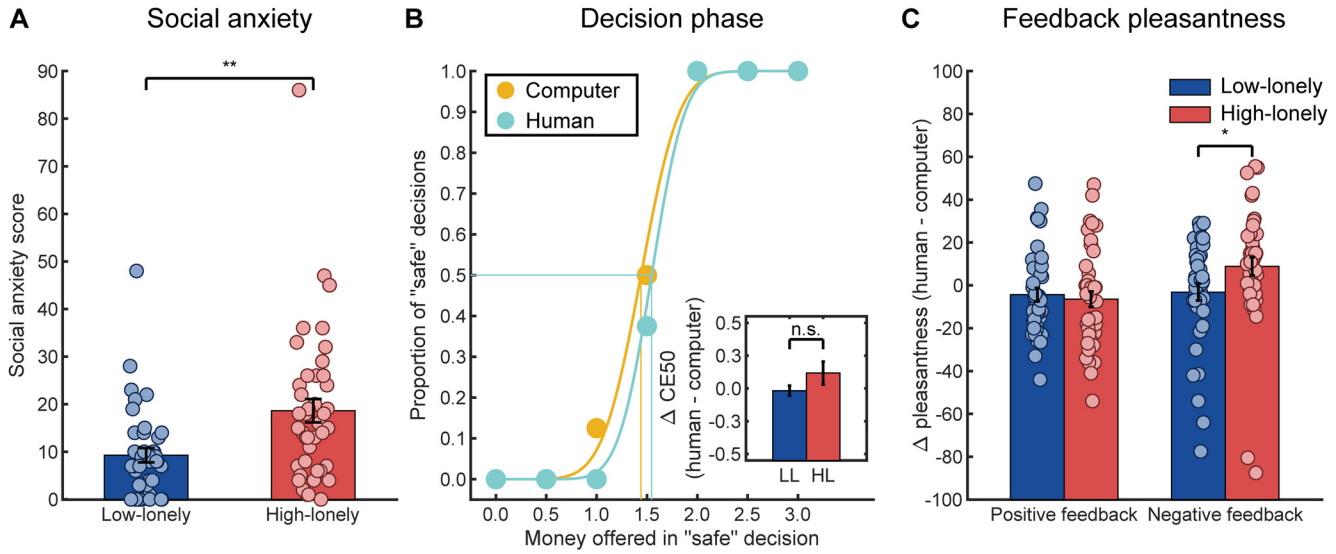

Figure 2. Behavioral results of the decision and feedback phase of the social gambling task. ***A***, Participants with HL showed significantly increased SA scores as assessed with the LSAS. ***B***, The proportion of safe decisions during the social gambling task increased with higher payoffs offered in those safe decisions (main effect of offered payoff for the behavioral task: $F_{(2.95,236.14)} = 183.77$, $p < 0.001$, $\eta_p^2 = 0.70$; fMRI task: $F_{(2,158)} = 185.43$, $p < 0.001$, $\eta_p^2 = 0.70$; example data of the behavioral task from 1 HL participant are presented). As presented in the inlay, HL participants did not significantly differ from participants with LL with regard to the subjective value of engaging in a social situation (i.e., CE50, the payoff offered in the safe option associated with 50% of safe decisions; $t_{(47.81)} = 1.42$, $p = 0.16$, Bayes factor [BF_{10}] = 0.57). ***C***, By contrast, groups significantly differed in their pleasantness ratings of the negative feedback videos. Compared with the negative computer feedback video, HL participants rated the negative human feedback video as more pleasant, whereas LL participants showed the opposite pattern of ratings. No differences between groups were observed for positive feedback. Each marker in ***B*** represents the mean of 8 trials. Bars represent group means. Error bars indicate SEM. *$p < 0.05$. **$p < 0.01$. n.s., not significant.

participants could be explained by increased SA in HL participants. Therefore, mediation analyses were calculated with group serving as independent variable and SA serving as mediator.

To examine the influence of further possible confounding variables on significant group effects (i.e., depressive symptomatology assessed by the Beck's Depression Inventory II [BDI], Beck et al., 1996; and childhood maltreatment assessed by the Childhood Trauma Questionnaire [CTQ], Bernstein et al., 1994), we calculated mediation and moderation analyses using the PROCESS macro version 3.4 for SPSS (Hayes, 2017). BDI and CTQ scores were used as mediator and moderator variables and group as predictor variable. Again, mediation analyses were calculated to examine whether observed differences between groups might be driven by differences in psychiatric symptomatology, whereas moderation analyses were conducted to investigate a potential interaction of loneliness (HL vs LL) with the moderation variable. For mediation analyses, 10,000 bootstrap samples were used. Variables were mean-centered before calculating moderation analyses. Mediations were considered significant if the 95% CI of an indirect effect excluded zero, while moderations were considered significant if $p < 0.05$ for the interaction effect of group with the potential moderator. Moreover, we further examined whether the observed effects of group remained significant ($p < 0.05$ for the direct effect of group) after including the potential confounding variables (SA, BDI, and CTQ scores) as covariates in the regression model to probe the robustness of the observed explorative loneliness-related findings.

Results

Behavioral results

As expected, SA was significantly increased in HL participants ($t_{(67.74)} = 3.25$, $p = 0.002$, $d = 0.72$; mean LSAS score ± SD in HL: 18.64 ± 15.91, range: 0-86; LL: 9.28 ± 9.56, range: 0-48; Fig. 2*A*) (Lieberz et al., 2021), and task effects of the social gambling task reported by Schultz et al. (2019) were replicated across groups: the proportion of safe decisions in the behavioral social gambling task significantly increased with higher payoffs offered as safe alternative to the risky gambling decision across groups (main effect of offered payoff: $F_{(2.95,236.14)} = 183.77$, $p < 0.001$, $\eta_p^2 = 0.70$; Fig. 2*B*) and was highest for an offered payoff of 3 € (mean proportion of safe decisions ± SD for an offered payoff of 0 €: 8.16 ± 17.06%; 0.5 €: 8.38 ± 16.44%; 1 €: 19.36 ± 28.44%; 1.5 €: 37.96 ± 36.12%; 2 €: 76.98 ± 30.70%; 2.5 €: 84.98 ± 25.85%; 3 €: 88.11 ± 23.48%). Likewise, the proportion of safe decisions differed between all three payoffs offered during the fMRI implementation of the task (main effect of offered payoff: $F_{(2,158)} = 185.43$, $p < 0.001$, $\eta_p^2 = 0.70$; *post hoc* comparisons: CE20 vs CE50: $t_{(80)} = 8.27$, $p_{cor} < 0.001$, $d = 1.08$; CE50 vs CE80: $t_{(80)} = 11.02$, $p_{cor} < 0.001$, $d = 1.44$; mean proportion of safe decisions ± SD for an offered payoff of CE20: 12.13 ± 18.91%; CE50: 41.57 ± 32.27%; CE80: 82.30 ± 22.69%). Importantly, as individual payoffs were calculated for the fMRI task separately for human and computer partners to equalize the ratio of risky and safe decisions, the likelihood of safe decisions during fMRI differed neither between partners nor between groups (HL vs LL) (all main effects or interactions of the partner condition or group F values < 1.48, p values > 0.05). As intended, positive feedback videos were rated as more pleasant than negative ones (main effect of feedback valence: $F_{(1,80)} = 174.73$, $p < 0.001$, $\eta_p^2 = 0.69$). SA was indeed negatively associated with the subjective value of engaging in social situations in the LL group, but the correlation failed to reach significance ($r_{(38)} = -0.22$, $p = 0.21$).

However, contrary to previously observed effects of SA (Schultz et al., 2019), loneliness (HL vs LL) affected neither the subjective value of engaging in social situations during the behavioral social gambling task nor investments in the virtual auction task (all p values > 0.05). Nevertheless, analyses of pleasantness ratings of the feedback videos revealed a significant interaction of group × partner × feedback valence ($F_{(1,80)} = 4.02$, $p = 0.048$, $\eta_p^2 = 0.05$). To disentangle the interaction, we calculated further mixed-design ANOVAs separately for the positive and negative feedback videos. Surprisingly, no group effects were observed for positive feedback (all p values > 0.05), but we found a significant interaction of group

× partner for negative feedback ($F_{(1,80)} = 4.34$, $p = 0.04$, $\eta_p^2 = 0.05$; Fig. 2*C*): HL participants rated the negative human feedback as more pleasant compared with the negative computer feedback ($t_{(41)} = 2.09$, $p_{cor} = 0.09$), while LL participants showed the opposite pattern of ratings ($t_{(39)} = -0.82$, $p_{cor} = 0.84$). Two additional explorative *post hoc* tests indicated that HL participants rated the negative computer feedback as less pleasant compared with LL participants (HL vs LL: $t_{(80)} = -2.09$, $p_{cor} = 0.08$; mean pleasantness ratings ± SD in HL participants: 25.91 ± 22.94; LL: 36.85 ± 24.38), whereas group differences vanished when negative feedback was provided by a human partner ($t_{(80)} = 0.34$, $p_{cor} \approx 1.00$; mean pleasantness ratings ± SD in HL participants: 34.77 ± 15.28; LL: 33.68 ± 14.29).

fMRI results

Multivariate and univariate analyses of neural activation across groups replicated all previous task effects (Schultz et al., 2019). As such, a linear support vector machine classifier based on amygdala activation was able to decode the decision (risky vs safe) significantly better than chance (mean accuracy ± SD = 53.64 ± 9.07%; 30, −4, 28, $t_{(73)} = 3.45$, $p_{FWE} = 0.048$). Amygdala activation increased during decisions involving a human partner compared with the computer partner (right: 22, −6, −12, $t_{(73)} = 3.68$, $p_{FWE} = 0.03$; left: −22, −8, −12, $t_{(73)} = 4.00$, $p_{FWE} = 0.01$). Specifically, amygdala activity was enhanced during trials in which participants chose the risky option with a human partner compared with the computer partner (right: 22, −6, −12, $t_{(73)} = 4.58$, $p_{FWE} = 0.002$; left: −22, −8, −12, $t_{(73)} = 4.23$, $p_{FWE} = 0.006$; Fig. 3*A*), while no differences in amygdala activity between partners were observed for safe decisions. Moreover, receiving feedback from the human partner activated the amygdala significantly stronger than computer feedback (right: 22, −6, −14, $t_{(75)} = 9.67$, $p_{FWE} < 0.001$, left: −22, −8, −12, $t_{(75)} = 9.66$, $p_{FWE} < 0.001$), and NAcc activity was increased in response to positive feedback compared with negative feedback across partner types (right: 12, 8, −6, $t_{(75)} = 6.45$, $p_{FWE} < 0.001$, left: −14, 10 −10, $t_{(75)} = 4.91$, $p_{FWE} < 0.001$). Notably, while we found no association between SA and feedback processing, we were able to replicate the previously observed association between SA and amygdala hyperactivity during social decision-making in the LL group (SA scores correlated with right amygdala activity for risky decision human > risky decision computer: $r_{(35)} = 0.41$, $p = 0.01$; risky decision human > safe decision human: $r_{(35)} = 0.44$, $p = 0.007$). For whole-brain task effects, see Tables 1 and 2.

Importantly, however, neither amygdala activation during the decision or feedback stage nor the accuracy of decoding risky versus safe decisions based on amygdala activation patterns significantly differed between HL and LL participants. Conversely, we observed significant differences in striatal responses to the feedback videos: HL participants showed significantly smaller NAcc responses to human (vs computer) feedback than LL individuals (14, 14, −10, $t_{(74)} = 3.07$, $p_{FWE} = 0.02$). Again, the group difference was specific for negative feedback (14, 14, −10, $t_{(74)} = 3.21$, $p_{FWE} = 0.01$; Fig. 3*B*), whereas no significant group effects were observed for responses to positive feedback. *Post hoc* tests revealed increased NAcc responsiveness to negative human feedback compared with the computer feedback in LL participants ($t_{(36)} = 2.59$, $p_{cor} = 0.03$, $d = 0.53$), while HL participants exhibited the opposite response pattern ($t_{(38)} = -1.96$, $p_{cor} = 0.12$). In line with the behavioral results, further explorative *post hoc* tests indicated that group differences were based on a significantly enhanced NAcc responsiveness to the negative computer feedback in HL participants (HL vs LL: $t_{(74)} = 2.80$, $p_{cor} = 0.01$, $d = 0.62$), whereas group differences showed the opposite tendency for responses to negative human feedback ($t_{(74)} = -0.98$, $p_{cor} = 0.64$). No further group differences in brain activity were observed.

Exploratory gPPI analyses of the negative feedback condition with the NAcc serving as seed region indicated enhanced functional connectivity of the left NAcc with a cluster including the hippocampus in HL compared with LL participants (−14, −22, −14, $k = 73$, $t_{(74)} = 5.38$, $p_{FWE} = 0.049$ on cluster level; Fig. 4). Again, *post hoc* tests revealed an opposing pattern between groups when receiving negative human (vs computer) feedback: enhanced connectivity in HL participants ($t_{(38)} = 3.06$, $p_{cor} = 0.01$, $d = 0.63$) but reduced connectivity in LL participants ($t_{(36)} = -4.93$, $p_{cor} < 0.001$, $d = -1.15$). Two further *post hoc* comparisons again revealed differences between groups for negative computer feedback as functional connectivity was significantly reduced in HL participants (HL vs LL: $t_{(74)} = -4.62$, $p_{cor} < 0.001$, $d = 1.06$), whereas the involvement of a human partner reversed this pattern with significantly increased functional connectivity in HL participants (HL vs LL: $t_{(74)} = 2.40$, $p_{cor} = 0.04$, $d = 0.55$). Interestingly, NAcc-hippocampus connectivity not only correlated with NAcc responses to negative human feedback (contrasted with negative computer feedback: $r_{(74)} = -0.33$, $p = 0.004$, i.e., increased connectivity was associated with reduced neural reactivity), but also with pleasantness ratings of negative feedback videos ($r_{(74)} = 0.23$, $p = 0.04$; Fig. 4). The correlation between NAcc activity and negative feedback ratings was similar but failed to reach significance ($r_{(74)} = -0.20$, $p = 0.09$).

Bayesian analyses

Bayesian analyses revealed moderate evidence for the absence of group differences in variables that have previously been associated with SA (compare Schultz et al., 2019), with our data being at least 3 times more likely under the null hypothesis (H0: no differences between groups) than under the alternative hypothesis (HL differ from LL participants in any direction). Specifically, Bayesian *t* tests revealed moderate evidence that HL participants indeed did not differ from LL participants regarding the pleasantness ratings of positive human feedback as our data were found to be almost 4 times more likely under the H0 than under the alternative hypothesis (Bayes factor (BF_{10}) = 0.25, median effect size = 0.08, 95% credible interval: [−0.32, 0.49]).

Likewise, Bayesian analyses revealed moderate evidence that groups showed equal reward-associated brain activity in response to positive human feedback (left NAcc: $BF_{10} = 0.25$, median effect size = 0.07, 95% credible interval: [−0.35, 0.49]; for the right NAcc, the evidence is inconclusive: $BF_{10} = 0.43$, median effect size = 0.23, 95% credible interval: [−0.19, 0.66]) and moderate evidence in favor of the H0 for amygdala reactivity to human feedback (left: $BF_{10} = 0.24$, median effect size = −0.004, 95% credible interval: [−0.42, 0.41]; right: $BF_{10} = 0.24$, median effect size ≈ 0.00, 95% credible interval: [−0.42, 0.42]). The same pattern of results was observed for amygdala activation during the decision stage of the social gambling task as our data were up to 4 times more likely under the assumption of comparable activation between groups (H0) than under the alternative hypothesis (left amygdala activation for risky decisions with a human partner compared with a computer partner: $BF_{10} = 0.24$, median effect size = 0.03, 95% credible interval: [−0.39, 0.45]; left amygdala activation for risky decisions with a human partner contrasted with safe decisions in trials with a human partner: $BF_{10} = 0.33$, median effect size = −0.17, 95% credible interval: [−0.61, 0.25]; right: $BF_{10} = 0.24$, median effect size = −0.01, 95% credible interval: [−0.43, 0.41]). For right amygdala activation, there was insufficient evidence to draw a conclusion for or against the

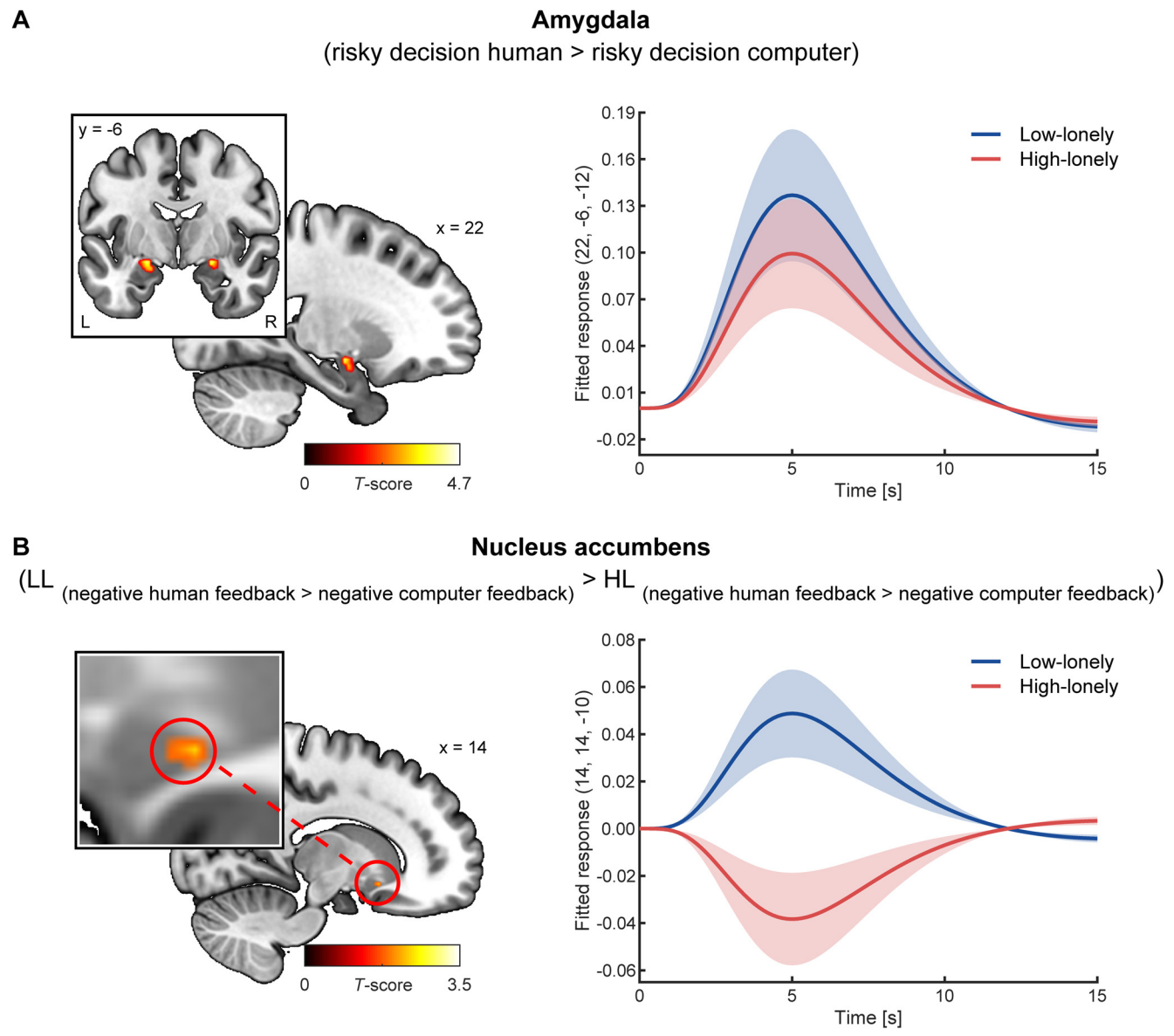

Figure 3. Neural activation during the social gambling task. ***A***, Amygdala activity was significantly enhanced during the decision phase of the social gambling task when participants chose the risky option with a human partner compared with the computer partner (right: 22, −6, −12, $t_{(73)} = 4.58$, $p_{FWE} = 0.002$; left: −22, −8, −12, $t_{(73)} = 4.23$, $p_{FWE} = 0.006$). In line with the behavioral results, no group differences in neural activity were observed during the decision phase. ***B***, During the feedback stage, participants with HL showed attenuated NAcc responses to negative feedback given by human partners compared with the computer partner. In contrast, NAcc reactivity to negative human feedback was enhanced compared with computer feedback in participants with LL. Shaded areas represent the SEM of the fitted responses based on the HRF. For illustration purpose, clusters are shown with significance levels of $p < 0.05$ uncorrected. L, left; R, right.

hypothesis that groups exhibit equal responsiveness to risky decisions involving a human partner (contrasted with the computer; $BF_{10} = 0.50$, median effect size = 0.26, 95% credible interval: [−0.16, 0.70]). However, descriptive analyses revealed an opposing response pattern in HL participants to what has been expected because of increased SA symptoms: while LL participants showed slightly enhanced amygdala activation (mean parameter estimates ± SD: 0.25 ± 1.06), amygdala activation was reduced in HL participants (mean parameter estimates ± SD: −0.02 ± 0.68; compare Fig. 3*A*). Likewise, no evidence for any of the hypotheses (null or alternative hypothesis) was observed for the subjective value of engaging in social situations ($BF_{10} = 0.57$, median effect size = −0.29, 95% credible interval = [−0.74, 0.15]). Again, descriptive analyses revealed enhanced values of social engagement in HL compared with LL participants, which is contrary to the previously reported negative association with SA (Fig. 2*B*, inlay) (compare Schultz et al., 2019).

Regarding the invested money during the virtual auction task, Bayesian analyses provided moderate evidence for comparable investments between groups to avoid negative human feedback ($BF_{10} = 0.33$, median effect size = 0.17, 95% credible interval = [−0.23, 0.59]) or to receive positive human feedback ($BF_{10} = 0.33$, median effect size = 0.18, 95% credible interval = [−0.23, 0.59]).

Interactions of loneliness with SA

To summarize, although HL individuals reported higher SA scores, loneliness was not associated with behavioral and neural correlates, which have been previously found to be affected by SA and which could be partially replicated in LL participants. We thus explored whether SA-related findings differed significantly between HL and

Table 1. Whole-brain findings during decision-making across groups[a]

Region	Right/left	Cluster size (voxel)	Peak *T*	MNI coordinates		
				x	*y*	*z*
Decision human > decision computer						
Medial orbitofrontal gyri	Bilateral	351	6.28	2	44	−14
Precuneus	Bilateral	800	6.04	4	−56	28
Risky decision > safe decision						
Inferior frontal gyrus, triangularis	R	2218	8.77	44	24	24
Middle occipital gyrus	L	588	7.65	−44	−68	4
Fusiform gyrus	L	249	7.29	−22	−80	−8
Middle temporal gyrus	R	452	6.77	42	−58	10
Lingual gyrus	R	595	6.60	4	−80	−4
Anterior cingulate cortex	Bilateral	331	6.26	8	−14	30
Precentral gyrus	L	557	6.15	−42	−6	48
Supplementary motor area	R	633	6.09	8	8	60
Supramarginal gyrus	R	313	6.07	44	−40	14
Superior parietal gyrus	L	203	5.99	−26	−52	48
Superior temporal gyrus	R	110	5.90	50	−22	−4
Inferior temporal gyrus	L	120	5.73	−40	−44	−14
Superior occipital gyrus	L	220	5.58	−14	−66	38
Insular cortex	L	214	5.47	−30	26	2
Inferior parietal gyrus	R	139	5.28	28	−52	52
Risky decision human > risky decision computer						
Superior temporal gyrus	R	448	7.60	48	−40	10
Precuneus	Bilateral	496	6.64	6	−56	28
Medial orbitofrontal gyri	Bilateral	328	5.79	2	42	−14
Inferior frontal gyrus, triangularis	R	315	5.49	42	16	22

[a]Cluster sizes are based on the initial cluster-forming height threshold of $p < 0.001$. Peak *T* and MNI coordinates are listed for FWE-corrected *p* values < 0.05 on peak level. No cluster survived the FWE correction on the peak level for the safe decision human > safe decision computer contrast.

Table 2. Whole-brain findings during the feedback phase across groups[a]

Region	Right/left	Cluster size (voxel)	Peak *T*	MNI coordinates		
				x	*y*	*z*
Human feedback > computer feedback						
Middle temporal gyrus	R	6837	12.07	54	−40	8
Calcarine fissure	R	141	12.01	22	−94	−2
Amygdala	L	3273	9.66	−22	−8	−12
Fusiform gyrus	R	361	9.29	40	−48	−16
Fusiform gyrus	L	296	8.44	−38	−48	−20
Middle occipital gyrus	L	32	7.65	−20	−94	−2
Gyri rectus	Bilateral	295	6.54	6	38	−16
Inferior occipital gyrus	R	42	5.29	44	−76	−6
Positive feedback > negative feedback						
Inferior occipital gyrus	R	341	8.32	26	−92	−2
Caudate nuclei	Bilateral	2792	8.10	8	10	−2
Middle cingulate gyri	Bilateral	2897	6.80	−2	−34	34
Inferior occipital gyrus	L	101	6.63	−28	−88	−6
Angular gyrus	L	3721	6.15	−40	−66	46
Middle frontal gyrus	L	2771	6.11	−30	16	52
Precentral gyrus	R	2059	5.62	36	−28	62
Superior frontal gyrus	R	722	5.59	20	34	48
Inferior orbitofrontal gyrus	L	55	5.53	−26	30	−16
Fusiform gyrus	L	229	5.43	−26	−46	−18
Positive human feedback > negative human feedback						
Caudate nuclei	Bilateral	685	7.52	8	10	−2
Angular gyrus	L	937	6.23	−40	−68	34
Middle temporal gyrus	R	1487	6.09	56	−36	6
Middle temporal gyrus	L	551	5.63	−58	−42	10
Middle temporal gyrus	L	280	5.47	−48	−70	6
Precentral gyrus	R	1087	5.31	40	−26	64

[a]Cluster sizes are based on the initial cluster-forming height threshold of $p < 0.001$. Peak *T* and MNI coordinates are listed for FWE-corrected *p* values < 0.05 on peak level. For the positive feedback > negative feedback contrast, the NAcc is included in the caudate nuclei cluster.

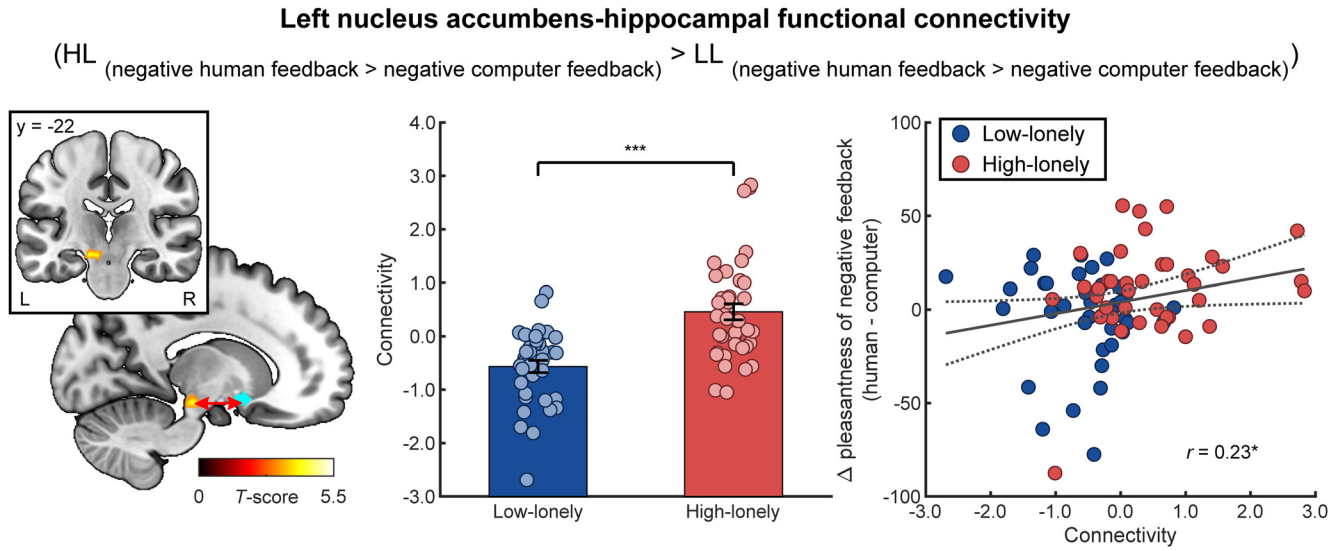

Figure 4. Functional connectivity during the social gambling task. Participants with HL showed enhanced functional connectivity of the NAcc (blue sphere) with a cluster including the hippocampus while receiving negative human (vs computer) feedback compared with participants with LL. Functional connectivity positively correlated with the pleasantness ratings of the negative human feedback (compared with the negative computer feedback). Dashed line indicates the 95% CI of the plotted regression line. Bars represent group means. Error bars indicate SEM. $^{*}p < 0.05$. $^{***}p < 0.001$. L, left; R, right.

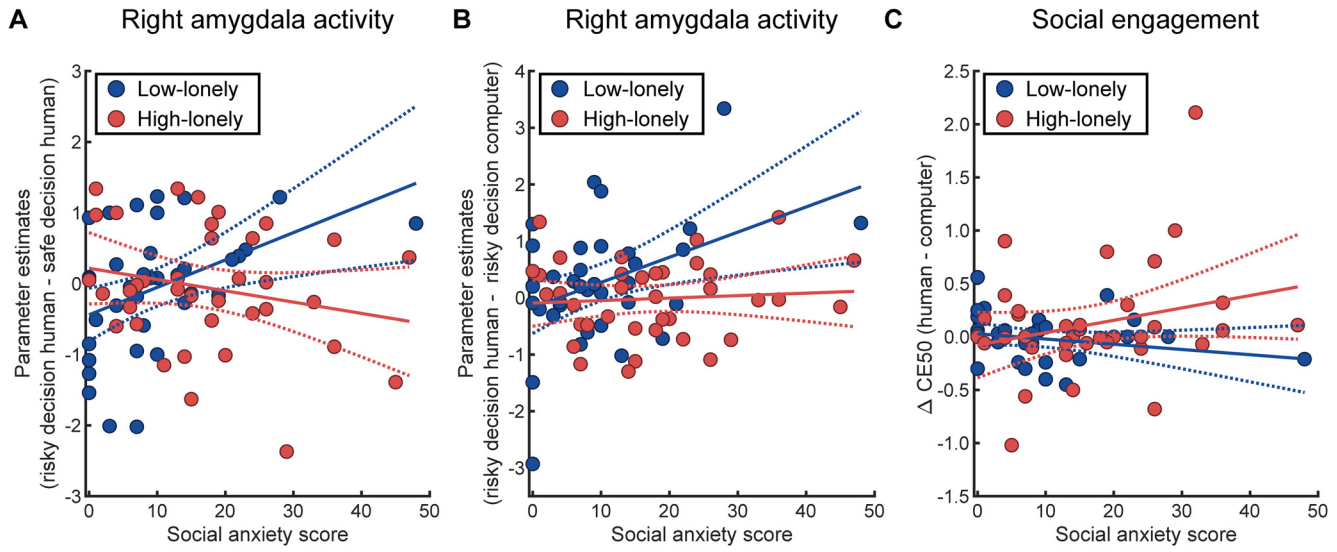

Figure 5. Interactions of loneliness with SA. ***A***, Moderation analyses revealed that the positive association of SA with right amygdala activation during risky social decision-making (risky decision human – safe decision human) as observed in participants with LL ($\beta = 0.63$, $p = 0.007$, 95% CI: [0.18, 1.08]) was not evident in participants with HL ($\beta = -0.26$, $p = 0.17$, 95% CI: [−0.63, 0.11]). ***B***, Likewise, the positive relationship of SA with right amygdala activation during social decision-making contrasted with risky decisions involving a computer partner vanished in the HL group (LL: $\beta = 0.69$, $p = 0.003$, 95% CI: [0.25, 1.14]; HL: $\beta = 0.07$, $p = 0.72$, 95% CI: [−0.30, 0.43]). ***C***, Moreover, the nonsignificant negative association of SA with the subjective value of engaging in a social situation (i.e., CE50, the payoff offered in the safe option associated with 50% of safe decisions) in the LL group ($\beta = -0.17$, $p = 0.48$, 95% CI: [−0.64, 0.30]) was reversed in the HL group ($\beta = 0.40$, $p = 0.049$, 95% CI: [0.002, 0.80]). Thus, higher SA symptomatology was even associated with increased subjective values of engaging in social situations for participants suffering from loneliness. Dashed lines indicate the 95% CI of the plotted regression lines.

LL participants. Indeed, moderation analyses revealed that SA-related effects on amygdala activation during social decision-making were significantly different for HL compared with LL participants (interaction of SA with group for right amygdala activation during risky decisions with a human partner compared with safe decisions with a human partner: $\beta = -0.88$, $t_{(70)} = -3.02$, $p = 0.004$, 95% CI: [−1.47, −0.30]; for right amygdala activation during risky decisions with a human partner compared with risky decisions with the computer partner: $\beta = -0.63$, $t_{(70)} = -2.16$, $p = 0.03$, 95% CI: [−1.20, −0.05]; Fig. 5*A*,*B*). As already reported (see fMRI results), SA was positively associated with the average activation across all voxels of the right amygdala for risky decisions involving a human partner (compared with safe decisions involving a human partner: $\beta = 0.63$, $p = 0.007$, 95% CI: [0.18, 1.08]; compared with risky decisions involving the computer: $\beta = 0.69$, $p = 0.003$, 95% CI: [0.25, 1.14]) in LL participants. Conversely, this association vanished in the HL group (risky decisions involving a human partner vs safe decisions involving a human partner: $\beta = -0.26$, $p = 0.17$, 95% CI: [−0.63, 0.11]; risky decisions involving a human partner vs risky decisions involving a computer partner: $\beta = 0.07$, $p = 0.72$, 95% CI: [−0.30, 0.43]). Moreover, moderation analyses indicated that the association of SA with the subjective values of engaging in social situations

might be altered in HL participants (interaction of SA with group: $\beta = 0.57$, $t_{(67)} = 1.84$ $p = 0.07$, 95% CI: [−0.05, 1.18]; Fig. 5*C*). As such, the reported nonsignificant negative association of SA with the social engagement in the LL group ($\beta = -0.17$, $p = 0.48$, 95% CI: [−0.64, 0.30]; see also Behavioral results) was reversed in the HL group ($\beta = 0.40$, $p = 0.049$, 95% CI: [0.002, 0.80]). Thus, higher SA symptomatology was significantly associated with increased subjective values of engaging in social situations for participants suffering from loneliness.

We then probed whether the differences between HL and LL participants were based on increased SA score in HL participants or whether loneliness effects on the processing of negative feedback differed for participants with high or low SA scores. Importantly, the observed effects of loneliness (HL vs LL) on NAcc responsiveness to negative human feedback (vs negative computer feedback) and on the NAcc-hippocampal functional connectivity while receiving negative feedback remained significant after including SA scores as covariate in the regression models (p values < 0.01 for all direct effects of group after including SA). Furthermore, no significant interactions between group and SA were observed, indicating that an altered processing of negative feedback in HL participants was not enhanced or diminished by increased SA symptomatology. Finally, we explored whether the altered feedback processing in HL participants was driven by increased SA by calculating mediation analyses with SA scores as potential mediator. Results revealed that none of the reported group effects was driven by SA. Conversely, analyses showed a significant suppressor effect of SA on the relationship between group and NAcc responses (indirect effect of group on NAcc activity via SA: $\beta = 0.14$, SE = 0.10, 95% CI: [0.005, 0.40]). Thus, the absolute height of the group effect even increased after including SA as mediator (effect of group without taking SA into account: $\beta = -0.69$, SE = 0.22, 95% CI: [−1.12, −0.26]; with SA as mediator: $\beta = -0.83$, SE = 0.23, 95% CI: [−1.28, −0.38]; for NAcc-hippocampal functional connectivity and pleasantness ratings of negative human vs computer feedback, 95% CIs included zero for the SA mediator effect; i.e., the indirect effect of group via SA).

Effects of further confounding variables

Groups differed significantly regarding psychiatric symptoms (compare Lieberz et al., 2021). In addition to increased SA symptomatology, HL participants reported more depressive symptoms ($t_{(50.89)} = 4.15$, $p < 0.001$, $d = 0.92$; mean BDI score ± SD in HL: 6.62 ± 6.76; LL: 2.03 ± 2.31) and more severe childhood maltreatment ($t_{(80)} = 2.38$, $p = 0.02$, $d = 0.53$; mean CTQ score ± SD in HL: 38.86 ± 10.28; LL: 31.90 ± 15.76). Importantly, as reported for SA, the observed effects of loneliness (HL vs LL) on NAcc responsiveness to negative human feedback remained significant after including the depression or childhood maltreatment as covariates in the regression models (p values < 0.01 for all direct effects of group after including the potential confounding variables). Likewise, loneliness effects on NAcc-hippocampal functional connectivity while receiving negative human feedback were found to be robust (all direct effects of group after including the potential confounding variables p values < 0.0001). Mediation and moderation analyses indicated that none of the reported group effects was mediated or moderated by confounding psychiatric symptoms (the 95% CI of all tested indirect effects included zero and all interaction effects of group with the potential moderator p values > 0.05).

Discussion

The current study sought to investigate shared and distinct behavioral and neural response patterns underlying SA and liness. While we were able to replicate previously reported task effects and SA-related amygdala hyperactivation during social decision-making (compare Schultz et al., 2019), our results revealed that a previously observed neurocircuitry underlying avoidance behavior in SA is not evident in lonely individuals. HL participants differed from LL participants neither in the subjective value of engaging in social situations nor in neural responses to social decision-making and positive social feedback. Moreover, the association of SA symptomatology with increased amygdala activation during social decision-making vanished in HL participants. Conversely, the previously reported association of higher SA with reduced subjective values of engaging in social situations was even reversed in HL participants. Further explorative analyses indicated that HL participants showed an altered responsiveness to negative computer feedback as evident in reduced pleasantness ratings and increased striatal activity, which was normalized when negative feedback was provided by a human partner. Moreover, striatal-hippocampal functional connectivity in HL participants, which was diminished while receiving negative computer feedback, was significantly increased during negative social feedback.

Our results indicate that neural and behavioral correlates of loneliness differ from a socially avoidant phenotype associated with SA. Loneliness did not significantly correlate with behavioral tendencies to withdraw from social interactions in the current study. Human and animal research has consistently shown that the amygdala is crucially involved in the processing of threat-related stimuli, and hyperactivation of the amygdala is known as a core mechanism underlying anxiety disorders (Phelps and LeDoux, 2005; Etkin and Wager, 2007). Moreover, amygdala habituation to threat-related stimuli and amygdala connectivity with prefrontal regions predict subsequent avoidance behavior (Björkstrand et al., 2020; Lisk et al., 2020; Mao et al., 2020). Likewise, we have previously found that amygdala activation during decisions in the social gambling task increases with SA symptomatology and negatively correlates with the subjective value to engage in social situations (Schultz et al., 2019). By contrast, the subjective value of engaging in a social situation did not differ between HL and LL participants, and Bayesian analyses revealed evidence for comparable amygdala activation during the decision and feedback stages. Moreover, the link between amygdala activation during social decision-making and SA symptoms differed significantly between HL and LL participants, thus providing further support for the heterogeneity in clinical phenotypes and underlying biotypes of SA (Spokas and Cardaciotto, 2014; Williams, 2017). In line with our findings, neuroanatomical correlates of social avoidance behavior were previously found to be unaffected by loneliness (Tian et al., 2016). This notion is consistent with etiologic theories that highlight maladaptive social cognitions in the development and maintenance of loneliness (Spithoven et al., 2017; Cacioppo and Cacioppo, 2018). Likewise, cognitive-behavioral interventions were found to be more effective in targeting social biases than social skill trainings (Masi et al., 2011; Veronese et al., 2021). There is preliminary evidence that established cognitive-behavioral treatments targeting SA concurrently decrease feelings of loneliness and vice versa (Alfano et al., 2009; Suveg et al., 2017; Haslam et al., 2019; Käll et al., 2021; O'Day et al., 2021), but our findings of distinct behavioral and neural substrates suggest that loneliness-adjusted protocols might improve therapeutic outcomes.

Moreover, our explorative results provide new insights into the neural pathways underlying loneliness. Unexpectedly, striatal

activity during negative social feedback was reduced while pleasantness ratings were increased in HL participants. Notably, activation of the NAcc is associated with goal-directed approach and avoidance behavior and involved in avoiding social punishment (Kohls et al., 2013; Damiano et al., 2015; Floresco, 2015). Furthermore, our results are in line with parcellation studies highlighting specific roles of the ventral-caudal NAcc shell and the rostral, core-like NAcc. The former has been associated with reward anticipation and reward processing, while activation of the latter may also reflect the processing of negative events (Baliki et al., 2013; Xia et al., 2017; Oldham et al., 2018). Concordantly, the observed group differences in response to negative feedback were restricted to rostral, core-like parts of the NAcc, whereas positive feedback activated both rostral and caudal parts of the NAcc across groups. As HL participants rated the negative social feedback videos as more pleasant than the negative computer feedback, reduced core-like NAcc responses to negative social feedback might thus reflect reduced tendencies to avoid this negative social feedback. Conversely, the opposite pattern of results was observed for LL participants. Furthermore, the enhanced functional coupling of the NAcc with a hippocampal cluster that correlated with individual pleasantness ratings is in line with the involvement of this neural circuit in hedonic processing (Yang et al., 2020) and might reflect the rewarding experience of a social feedback for socially deprived individuals (Tomova et al., 2020). As such, our results indicate that HL participants might be more affected by negative events compared with LL participants. The involvement of another human, however, might attenuate this bias. Nevertheless, we have recently found a compromised neural integration of social information in HL participants evident in various brain regions, including the NAcc (Lieberz et al., 2021). Furthermore, loneliness has been associated with a reduced recognition of negative vocal expressions (Morningstar et al., 2020). Thus, the reduced NAcc activity might also reflect diminished differentiation between positive and negative feedback, resulting in a dysregulated reward system responsiveness to negative social stimuli as observed for the NAcc-hippocampus connectivity. However, inference about cognitive processes from neural activation should always be drawn with restraint (Poldrack, 2006), and results regarding biased emotion recognition in loneliness are inconclusive (Spithoven et al., 2017). Future studies are warranted to further investigate the impact of loneliness on the processing of negative events in general and on the processing of negative social feedback in particular. For instance, implementing representational similarity analyses and incorporating multimodal data might help to understand how negative social feedback is represented in HL participants, how its processing contributes to future behavior, and whether its neural representation differs from LL individuals or from patients suffering from SA.

Interestingly, differences between HL and LL participants were restricted to behavioral and neural responses to negative social feedback, whereas Bayesian analyses revealed evidence for a comparable responsiveness to positive social feedback between groups. Conversely, SA has been consistently found to affect the processing of social rewards (Sripada et al., 2013; Richey et al., 2014, 2017; Schultz et al., 2019). Previous studies point to various negative effects of loneliness on the processing of positive social interactions (Cacioppo et al., 2009; Silva et al., 2017; Lieberz et al., 2021), but findings about the association between loneliness and NAcc reactivity to positive social stimuli are mixed. The involvement of the NAcc in loneliness might be context-dependent, with feelings of social isolation promoting the hedonic experience of positive social stimuli in an acute stage (Tomova et al., 2020), which may be different from chronic loneliness (Saporta et al., 2021). Similarly, lonely individuals might experience a social stimulus as more rewarding only if the stimulus is already familiar (e.g., a romantic partner and not a stranger) (Inagaki et al., 2016). Along these lines, a recent study found no relationship of loneliness with striatal responsiveness to pictures depicting strangers during positive social interactions (D'Agostino et al., 2018). Nevertheless, in our task design, positive feedback was always coupled with monetary gains. Thus, differences regarding positive social feedback might have been obfuscated by the rewarding experience of earning money as evident in enhanced striatal responsiveness to positive feedback, regardless of the partner providing the feedback. Both external (e.g., passive viewing vs being involved in positive social interactions) and internal factors (e.g., state vs chronic feelings of social isolation) may influence the association of loneliness with social reward processing.

Moreover, given the quasi-experimental, cross-sectional design of our study, our findings do not allow casual inferences about the relationship of loneliness and social feedback processing. Additionally, analyses indicate that the observed associations with loneliness were not driven by psychiatric symptoms that were also more pronounced in HL individuals. However, our study specifically focused on high-lonely healthy individuals who may represent a resilient subsample of the population because they did not develop acute psychiatric disorders. Thus, clinical studies with psychiatric patients are warranted to uncover the direction of the observed associative relationships and to further disentangle shared and distinct mechanisms underlying loneliness and psychopathology. Likewise, we cannot exclude the possibility that the LL group may also represent a special, hypersocial group, that differs from the average population. Nevertheless, previous studies indicated that the intensity of loneliness matters mostly for individuals with high loneliness, whereas differences in the experience of loneliness between low and medium lonely individuals had no effect on loneliness-related hypervigilance for social threats (Qualter et al., 2013). While it thus seems unlikely that the inclusion of an intermediate group with average loneliness scores would change the direction of the observed group differences, it might still be of great interest for future studies to investigate clinically relevant cutoff points in either direction. This way, research might help to identify individuals who are at high risk for mental and physical health problems because of high loneliness and in turn to characterize protective mechanisms of highly social individuals that might prevent psychiatric disorders.

Collectively, the current results suggest that loneliness and SA are distinct constructs with specific behavioral and neural substrates. Along these lines, interventions targeting loneliness-specific cognitive biases may be more effective in reducing loneliness than cognitive-behavioral therapies focused on reducing avoidance behavior.

References

Alfano CA, Pina AA, Villalta IK, Beidel DC, Ammerman RT, Crosby LE (2009) Mediators and moderators of outcome in the behavioral treatment of childhood social phobia. J Am Acad Child Adolesc Psychiatry 48:945–953.

Baliki MN, Mansour A, Baria AT, Huang L, Berger SE, Fields HL, Apkarian AV (2013) Parceling human accumbens into putative core and shell dissociates encoding of values for reward and pain. J Neurosci 33:16383–16393.

Beck A, Steer RA, Brown GK (1996) Beck Depression Inventory-II. San Antonio, TX: Psychological Corporation.

Bernstein DP, Fink L, Handelsman L, Foote J, Lovejoy M, Wenzel K, Sapareto E, Ruggiero J (1994) Initial reliability and validity of a new retrospective measure of child abuse and neglect. Am J Psychiatry 151:1132–1136.

Björkstrand J, Agren T, Frick A, Hjorth O, Furmark T, Fredrikson M, Åhs F (2020) Decrease in amygdala activity during repeated exposure to spider images predicts avoidance behavior in spider fearful individuals. Transl Psychiatry 10:292.

Bruce LD, Wu JS, Lustig SL, Russell DW, Nemecek DA (2019) Loneliness in the United States: a 2018 national panel survey of demographic, structural, cognitive, and behavioral characteristics. Am J Health Promot 33:1123–1133.

Bruhl AB, Delsignore A, Komossa K, Weidt S (2014) Neuroimaging in social anxiety disorder: a meta-analytic review resulting in a new neurofunctional model. Neurosci Biobehav Rev 47:260–280.

Cacioppo JT, Cacioppo S (2018) Loneliness in the modern age: an evolutionary theory of loneliness (ETL). In: Advances in experimental social psychology (Olson JM, ed), pp 127–197. Cambridge, MA: Academic.

Cacioppo JT, Norris CJ, Decety J, Monteleone G, Nusbaum H (2009) In the eye of the beholder: individual differences in perceived social isolation predict regional brain activation to social stimuli. J Cogn Neurosci 21:83–92.

Cacioppo JT, Hawkley LC, Thisted RA (2010) Perceived social isolation makes me sad: 5-year cross-lagged analyses of loneliness and depressive symptomatology in the Chicago Health, Aging, and Social Relations Study. Psychol Aging 25:453–463.

Cho JW, Korchmaros A, Vogelstein JT, Milham MP, Xu T (2021) Impact of concatenating fMRI data on reliability for functional connectomics. Neuroimage 226:117549.

Clark DM, Wells A (1995) A cognitive model of social phobia. In: Social phobia: diagnosis, assessment, and treatment (Heimberg RG, Liebowitz MR, Hope DA, Schneider FR, eds), pp 69–94. New York: Guilford.

D'Agostino AE, Kattan D, Canli T (2018) An fMRI study of loneliness in younger and older adults. Soc Neurosci 14:136–148.

Damiano CR, Cockrell DC, Dunlap K, Hanna EK, Miller S, Bizzell J, Kovac M, Turner-Brown L, Sideris J, Kinard J, Dichter GS (2015) Neural mechanisms of negative reinforcement in children and adolescents with autism spectrum disorders. J Neurodev Disord 7:12.

Danneel S, Nelemans S, Spithoven A, Bastin M, Bijttebier P, Colpin H, Van Den Noortgate W, Van Leeuwen K, Verschueren K, Goossens L (2019) Internalizing problems in adolescence: linking loneliness, social anxiety symptoms, and depressive symptoms over time. J Abnorm Child Psychol 47:1691–1705.

Etkin A, Wager TD (2007) Functional neuroimaging of anxiety: a meta-analysis of emotional processing in PTSD, social anxiety disorder, and specific phobia. Am J Psychiatry 164:1476–1488.

Faul F, Erdfelder E, Lang AG, Buchner A (2007) G*Power 3: a flexible statistical power analysis program for the social, behavioral, and biomedical sciences. Behav Res Methods 39:175–191.

Floresco SB (2015) The nucleus accumbens: an interface between cognition, emotion, and action. Annu Rev Psychol 66:25–52.

Galea S, Merchant RM, Lurie N (2020) The mental health consequences of COVID-19 and physical distancing: the need for prevention and early intervention. JAMA Intern Med 180:817–818.

Haslam C, Cruwys T, Chang MX, Bentley SV, Haslam SA, Dingle GA, Jetten J (2019) GROUPS 4 HEALTH reduces loneliness and social anxiety in adults with psychological distress: findings from a randomized controlled trial. J Consult Clin Psychol 87:787–801.

Hayes AF (2017) Introduction to mediation, moderation, and conditional process analysis: a regression-based approach. New York: Guilford.

Hebart MN, Gorgen K, Haynes JD (2014) The Decoding Toolbox (TDT): a versatile software package for multivariate analyses of functional imaging data. Front Neuroinform 8:88.

Heinrich LM, Gullone E (2006) The clinical significance of loneliness: a literature review. Clin Psychol Rev 26:695–718.

Holt-Lunstad J, Smith TB, Layton JB (2010) Social relationships and mortality risk: a meta-analytic review. PLoS Med 7:e1000316.

Inagaki TK, Muscatell KA, Moieni M, Dutcher JM, Jevtic I, Irwin MR, Eisenberger NI (2016) Yearning for connection? Loneliness is associated with increased ventral striatum activity to close others. Soc Cogn Affect Neurosci 11:1096–1101.

JASP Team (2020) JASP (version 0.14.1). [Computer software]. Available at https://jasp-stats.org/.

Jeste DV, Lee EE, Cacioppo S (2020) Battling the modern behavioral epidemic of loneliness: suggestions for research and interventions. JAMA Psychiatry 77:553–554.

Käll A, Bäck M, Welin C, Åman H, Bjerkander R, Wänman M, Lindegaard T, Berg M, Moche H, Shafran R, Andersson G (2021) Therapist-guided internet-based treatments for loneliness: a randomized controlled three-arm trial comparing cognitive behavioral therapy and interpersonal psychotherapy. Psychother Psychosom 90:351–358.

Kashdan TB, Collins RL (2010) Social anxiety and the experience of positive emotion and anger in everyday life: an ecological momentary assessment approach. Anxiety Stress Coping 23:259–272.

Kaulard K, Cunningham DW, Bulthoff HH, Wallraven C (2012) The MPI facial expression database: a validated database of emotional and conversational facial expressions. PLoS One 7:e32321.

Keysers C, Gazzola V, Wagenmakers EJ (2020) Using Bayes factor hypothesis testing in neuroscience to establish evidence of absence. Nat Neurosci 23:788–799.

Kohls G, Perino MT, Taylor JM, Madva EN, Cayless SJ, Troiani V, Price E, Faja S, Herrington JD, Schultz RT (2013) The nucleus accumbens is involved in both the pursuit of social reward and the avoidance of social punishment. Neuropsychologia 51:2062–2069.

Lam JA, Murray ER, Yu KE, Ramsey M, Nguyen TT, Mishra J, Martis B, Thomas ML, Lee EE (2021) Neurobiology of loneliness: a systematic review. Neuropsychopharmacology 46:1873–1887.

Lieberz J, Shamay-Tsoory SG, Saporta N, Esser T, Kuskova E, Stoffel-Wagner B, Hurlemann R, Scheele D (2021) Loneliness and the social brain: how perceived social isolation impairs human interactions. Adv Sci 8:2102076.

Liebowitz MR (1987) Social phobia. Mod Probl Pharmacopsychiatry 22:141–173.

Lim MH, Rodebaugh TL, Zyphur MJ, Gleeson JF (2016) Loneliness over time: the crucial role of social anxiety. J Abnorm Psychol 125:620–630.

Lisk S, Kadosh KC, Zich C, Haller SP, Lau JY (2020) Training negative connectivity patterns between the dorsolateral prefrontal cortex and amygdala through fMRI-based neurofeedback to target adolescent socially-avoidant behaviour. Behav Res Ther 135:103760.

Maes M, Nelemans SA, Danneel S, Fernández-Castilla B, Van den Noortgate W, Goossens L, Vanhalst J (2019) Loneliness and social anxiety across childhood and adolescence: multilevel meta-analyses of cross-sectional and longitudinal associations. Dev Psychol 55:1548–1564.

Maldjian JA, Laurienti PJ, Kraft RA, Burdette JH (2003) An automated method for neuroanatomic and cytoarchitectonic atlas-based interrogation of fMRI data sets. Neuroimage 19:1233–1239.

Maldjian JA, Laurienti PJ, Burdette JH (2004) Precentral gyrus discrepancy in electronic versions of the Talairach atlas. Neuroimage 21:450–455.

Mao Y, Zuo XN, Ding C, Qiu J (2020) OFC and its connectivity with amygdala as predictors for future social anxiety in adolescents. Dev Cogn Neurosci 44:100804.

Masi CM, Chen HY, Hawkley LC, Cacioppo JT (2011) A meta-analysis of interventions to reduce loneliness. Pers Soc Psychol Rev 15:219–266.

Mihalopoulos C, Le LK, Chatterton ML, Bucholc J, Holt-Lunstad J, Lim MH, Engel L (2020) The economic costs of loneliness: a review of cost-of-illness and economic evaluation studies. Soc Psychiatry Psychiatr Epidemiol 55:823–836.

Morningstar M, Nowland R, Dirks MA, Qualter P (2020) Loneliness and the recognition of vocal socioemotional expressions in adolescence. Cogn Emot 34:970–976.

Morr M, Liu X, Hurlemann R, Becker B, Scheele D (2022) Chronic loneliness: neurocognitive mechanisms and interventions. doi: 10.31234/osf.io/r4f9e.

O'Day EB, Butler RM, Morrison AS, Goldin PR, Gross JJ, Heimberg RG (2021) Reductions in social anxiety during treatment predict lower levels of loneliness during follow-up among individuals with social anxiety disorder. J Anxiety Disord 78:102362.

Oldham S, Murawski C, Fornito A, Youssef G, Yucel M, Lorenzetti V (2018) The anticipation and outcome phases of reward and loss processing: a neuroimaging meta-analysis of the monetary incentive delay task. Hum Brain Mapp 39:3398–3418.

Peplau LA, Caldwell MA (1978) Loneliness: a cognitive analysis. Essence 2:207–220.

Phelps EA, LeDoux JE (2005) Contributions of the amygdala to emotion processing: from animal models to human behavior. Neuron 48:175–187.
Poldrack RA (2006) Can cognitive processes be inferred from neuroimaging data? Trends Cogn Sci 10:59–63.
Porter E, Chambless DL (2014) Shying away from a good thing: social anxiety in romantic relationships. J Clin Psychol 70:546–561.
Quadt L, Esposito G, Critchley HD, Garfinkel SN (2020) Brain-body interactions underlying the association of loneliness with mental and physical health. Neurosci Biobehav Rev 116:283–300.
Qualter P, Rotenberg K, Barrett L, Henzi P, Barlow A, Stylianou M, Harris RA (2013) Investigating hypervigilance for social threat of lonely children. J Abnorm Child Psychol 41:325–338.
Rapee RM, Peters L, Carpenter L, Gaston JE (2015) The Yin and Yang of support from significant others: influence of general social support and partner support of avoidance in the context of treatment for social anxiety disorder. Behav Res Ther 69:40–47.
Richey JA, Rittenberg A, Hughes L, Damiano CR, Sabatino A, Miller S, Hanna E, Bodfish JW, Dichter GS (2014) Common and distinct neural features of social and non-social reward processing in autism and social anxiety disorder. Soc Cogn Affect Neurosci 9:367–377.
Richey JA, Ghane M, Valdespino A, Coffman MC, Strege MV, White SW, Ollendick TH (2017) Spatiotemporal dissociation of brain activity underlying threat and reward in social anxiety disorder. Soc Cogn Affect Neurosci 12:81–94.
Rodebaugh TL, Lim MH, Shumaker EA, Levinson CA, Thompson T (2015) Social anxiety and friendship quality over time. Cogn Behav Ther 44:502–511.
Ruff CC, Fehr E (2014) The neurobiology of rewards and values in social decision making. Nat Rev Neurosci 15:549–562.
Russell D, Peplau LA, Cutrona CE (1980) The revised UCLA Loneliness Scale: concurrent and discriminant validity evidence. J Pers Soc Psychol 39:472–480.
Saporta N, Scheele D, Lieberz J, Stuhr-Wulff F, Hurlemann R, Shamay-Tsoory SG (2021) Opposing association of situational and chronic loneliness with interpersonal distance. Brain Sci 11:1135.
Schultz J, Willems T, Gädeke M, Chakkour G, Franke A, Weber B, Hurlemann R (2019) A human subcortical network underlying social avoidance revealed by risky economic choices. Elife 8:e45249.
Shao R, Liu HL, Huang CM, Chen YL, Gao M, Lee SH, Lin C, Lee TMC (2019) Loneliness and depression dissociated on parietal-centered networks in cognitive and resting states. Psychol Med 50:2691–2701.
Sheehan DV, Lecrubier Y, Sheehan KH, Amorim P, Janavs J, Weiller E, Hergueta T, Baker R, Dunbar GC (1998) The Mini-International Neuropsychiatric Interview (M.I.N.I.): the development and validation of a structured diagnostic psychiatric interview for DSM-IV and ICD-10. J Clin Psychiatry 59:22–33.
Silva HD, Campagnoli RR, Mota BE, Araújo CR, Álvares RS, Mocaiber I, Rocha-Rego V, Volchan E, Souza GG (2017) Bonding pictures: affective ratings are specifically associated to loneliness but not to empathy. Front Psychol 8:1136.
Spithoven AW, Bijttebier P, Goossens L (2017) It is all in their mind: a review on information processing bias in lonely individuals. Clin Psychol Rev 58:97–114.
Spokas ME, Cardaciotto L (2014) Heterogeneity within social anxiety disorder. In: The Wiley Blackwell handbook of social anxiety disorder, pp 247–267. New York: Wiley.
Sripada C, Angstadt M, Liberzon I, McCabe K, Phan KL (2013) Aberrant reward center response to partner reputation during a social exchange game in generalized social phobia. Depress Anxiety 30:353–361.
Suveg C, Kingery JN, Davis M, Jones A, Whitehead M, Jacob ML (2017) Still lonely: social adjustment of youth with and without social anxiety disorder following cognitive behavioral therapy. J Anxiety Disord 52:72–78.
Teo AR, Lerrigo R, Rogers MA (2013) The role of social isolation in social anxiety disorder: a systematic review and meta-analysis. J Anxiety Disord 27:353–364.
Tian X, Hou X, Wang K, Wei D, Qiu J (2016) Neuroanatomical correlates of individual differences in social anxiety in a non-clinical population. Soc Neurosci 11:424–437.
Tomova L, Wang KL, Thompson T, Matthews GA, Takahashi A, Tye KM, Saxe R (2020) Acute social isolation evokes midbrain craving responses similar to hunger. Nat Neurosci 23:1597–1605.
Veronese N, Galvano D, D'Antiga F, Vecchiato C, Furegon E, Allocco R, Smith L, Gelmini G, Gareri P, Solmi M, Yang L, Trabucchi M, De Leo D, Demurtas J (2021) Interventions for reducing loneliness: an umbrella review of intervention studies. Health Soc Care Community 29:e89–e96.
Vindegaard N, Benros ME (2020) COVID-19 pandemic and mental health consequences: systematic review of the current evidence. Brain Behav Immun 89:531–542.
Williams LM (2017) Defining biotypes for depression and anxiety based on large-scale circuit dysfunction: a theoretical review of the evidence and future directions for clinical translation. Depress Anxiety 34:9–24.
Xia X, Fan L, Cheng C, Eickhoff SB, Chen J, Li H, Jiang T (2017) Multimodal connectivity-based parcellation reveals a shell-core dichotomy of the human nucleus accumbens. Hum Brain Mapp 38:3878–3898.
Yang AK, Mendoza JA, Lafferty CK, Lacroix F, Britt JP (2020) Hippocampal input to the nucleus accumbens shell enhances food palatability. Biol Psychiatry 87:597–608.